

Sediment transport prediction in sewer pipes during flushing operation

Montes, Carlos; Ortiz, Hachly; Vanegas, Sergio; Kapelan, Zoran; Berardi, Luigi; Saldarriaga, Juan

DOI

[10.1080/1573062X.2021.1948077](https://doi.org/10.1080/1573062X.2021.1948077)

Publication date

2021

Document Version

Accepted author manuscript

Published in

Urban Water Journal

Citation (APA)

Montes, C., Ortiz, H., Vanegas, S., Kapelan, Z., Berardi, L., & Saldarriaga, J. (2021). Sediment transport prediction in sewer pipes during flushing operation. *Urban Water Journal*, 19(1), 1-14.
<https://doi.org/10.1080/1573062X.2021.1948077>

Important note

To cite this publication, please use the final published version (if applicable).
Please check the document version above.

Copyright

Other than for strictly personal use, it is not permitted to download, forward or distribute the text or part of it, without the consent of the author(s) and/or copyright holder(s), unless the work is under an open content license such as Creative Commons.

Takedown policy

Please contact us and provide details if you believe this document breaches copyrights.
We will remove access to the work immediately and investigate your claim.

Sediment Transport Prediction in Sewer Pipes During Flushing Operation

Carlos Montes^{a*}, Hachly Ortiz^b, Sergio Vanegas^c, Zoran Kapelan^d, Luigi Berardi^e and
Juan Saldarriaga^f

^a*Department of Civil and Environmental Engineering, Universidad de los Andes, Bogotá,
Colombia; e-mail: cd.montes1256@uniandes.edu.co*

^b*Department of Civil and Environmental Engineering, Universidad de los Andes, Bogotá,
Colombia; e-mail: hv.ortiz@uniandes.edu.co*

^c*Department of Civil and Environmental Engineering, Universidad de los Andes, Bogotá,
Colombia; e-mail: sm.vanegas@uniandes.edu.co*

^d*Department of Water Management, Delft University of Technology, Delft, Netherlands;
e-mail: Z.Kapelan@tudelft.nl*

^e*Department of Engineering and Geology, Università degli Studi "G. d'Annunzio" Chieti,
Pescara, Italy; e-mail: luigi.berardi@unich.it*

^f*Department of Civil and Environmental Engineering, Universidad de los Andes, Bogotá,
Colombia; e-mail: jsaldarr@uniandes.edu.co*

^{*}Corresponding author; Correspondence address: Cra 1 Este No. 19A – 40 Bogota
(Colombia); Tel.: +57-1-339-49-49 (ext. 1765)

Sediment Transport Prediction in Sewer Pipes During Flushing Operation

Abstract

This paper presents a novel model for predicting the sediment transport rate during flushing operation in sewers. The model was developed using the Evolutionary Polynomial Regression Multi-Objective Genetic Algorithm (EPR-MOGA) methodology applied to new experimental data collected. Using the new model, a series of design charts were developed to predict the sediment transport rate and the required flushing operation time for several pipe diameters. Accurate results (i.e. sediment transport rates) were obtained when applied to a case study in a combined sewer pipe in Marseille, as reported in the literature. The novelty of the model is the inclusion of the pipe slope, the inflow “dam break” hydrograph, and the sediment properties as explanatory parameters. The new model can be used to predict flushing efficiency and design new flushing cleaning schedules in sewer systems.

Keywords: flushing efficiency; sediment transport; sewer cleansing; sewer flushing.

1. INTRODUCTION

Sediment deposition and accumulation are well-known issues in sewer systems modelling. The presence of permanent deposits of material at the bottom of sewer pipes produces several problems, such as reduced flow capacity and premature combined sewer overflows (Ashley et al. 2004; Rodríguez et al. 2012). Flushing waves, also known as surge flushing technique, have been identified as an efficient (Bong et al. 2016; Yang et al. 2019) and cost-effective (Campisano et al. 2019, 2007) method for solving these problems. It aims to remove the deposited sediments by generating waves, which are produced by the upstream storage and further discharge of water volumes. These flushing

waves increase the bottom shear stress and induce the scour and resuspension of the deposited material.

The above flushing technique has been applied in several case studies following operational and management practice guides (British Standard Institution, 2014; Fan, 2004; Hlavinek et al. 2005; NEIWPC, 2003) in countries such as Germany, France, the USA and the UK. As an example, Hlavinek et al. (2005) suggest flushing waves to remove settled deposits in sewers ranging from 100 mm to 1200 mm pipe diameter with a mandatory cleaning frequency once in 1 to 5 years. However, these guides do not specify important flushing parameters such as the hydraulic and pipe characteristics (i.e. length, slope and hydraulic roughness, among others), sediment properties and flushing volume. The lack of information on these specifications has contributed to the fact that existing flushing practices tend to be oversized. As an instance, Dettmar (2007) compared design tables developed by using extensive field studies and mathematical simulations (Chebbo et al. 1996; Dettmar, 2005; Lainé et al. 1998) and concluded that smaller flushing volumes and water storage heights achieve the same flushing length and efficiency in removing the volume of deposited sediments, compared to operational and management practice guides.

In the last decades, several studies have quantified the flushing efficiency in terms of: (a) reduction of volume and/or weight of sediments (Bong et al. 2016; Campisano et al. 2019, 2008, 2004; Creaco and Bertrand-Krajewski, 2009; Guo et al. 2004; Ristenpart, 1998; Shahsavari et al. 2017), (b) changes in deposited bed thickness (Bong et al. 2016, 2013a; Campisano et al. 2019, 2008, 2007, 2004; Dettmar et al. 2002; Ristenpart, 1998; Shahsavari et al., 2017; Shirazi et al. 2014), (c) variation of concentrations of total suspended solids (Ristenpart, 1998; Sakakibara, 1996), (d) increase in the bottom shear

stress (Bertrand-Krajewski et al. 2003; Campisano et al. 2008; Campisano and Modica, 2003; Dettmar et al. 2002; Ristenpart, 1998; Schaffner and Steinhardt, 2006; Yang et al. 2019), (e) length of the channel that can be potentially cleaned (Bertrand-Krajewski et al. 2003; Bong et al. 2013; Dettmar et al. 2002; Shahsavari et al. 2017; Yang et al. 2019) and (f) stored water volume discharged (Bertrand-Krajewski et al. 2003; Dettmar et al. 2002; Fan et al. 2001). These studies were carried out in both laboratory and real sewer flumes using different sediment characteristics, stored water volumes and geometrical characteristics of the flume. As a result, a list of parameters affecting the flushing efficiency was identified and classified in three main groups: (i) flushing hydraulics, (ii) pipe geometry and (iii) sediment properties. Flushing hydraulic parameters include water velocity (V_f), shear stress (τ), the water level in the pipe (Y), flowrate (Q), stored water head (h_o) and stored water volume discharged (V_a). In the pipe geometry, parameters as the slope (S_o), diameter (D), length (L), cross-section shape factor (β) and composite roughness (k_c) have been included. Finally, sediment properties include mean particle diameter (d), sediment thickness (y_s) and width (W_b), specific gravity (SG), porosity (η) and density (ρ_s).

The previous three groups of parameters have been used for implementing numerical models useful to quantify the flushing efficiency. Models found in the literature are focused on (i) solving complex mathematical structures, (ii) proposing simple dimensionless equations for estimating sediment transport rates and (iii) using Machine Learning (ML) and Artificial Intelligence (AI) techniques for finding patterns in data and predicting bedload and suspended load transport.

In the first approach, the one-dimensional Saint-Venant equations (Campisano et al. 2006; Campisano and Modica, 2003; De Sutter et al. 1999), coupled with the Exner

equation for uniform (Campisano et al. 2007, 2004; Creaco and Bertrand-Krajewski, 2009; Shirazi et al. 2014) and non-uniform (Campisano et al. 2019) sediments, are used for predicting bed sediment thickness changes during the flushing operation. More complex models involve the two-dimensional (Caviedes-Voullième et al. 2017; Yu and Duan, 2014) and three-dimensional (Schaffner and Steinhardt, 2006) solutions of the Saint-Venant equations. An example of the literature models is as follows:

$$\frac{\partial U}{\partial t} + \frac{\partial F(U)}{\partial x} = D(U) \quad (1)$$

where U , $F(U)$ and $D(U)$ are defined as follows:

$$U = \begin{bmatrix} A \\ Q \\ A_s \end{bmatrix}; F(U) = \begin{bmatrix} Q \\ V_f Q + \frac{F_h}{\rho} \\ \frac{1}{1-\rho} Q_s \end{bmatrix}; D(U) = \begin{bmatrix} 0 \\ gA \left(S_o - \frac{V_f^2}{k_c^2 R^{4/3}} \right) \\ 0 \end{bmatrix} \quad (2)$$

where F_h is the hydrostatic force over the cross-section, ρ the water density, R the hydraulic radius, A is the cross section wetted area, A_s is the cross-section sediment bed area and Q_s the sediment flow rate.

In the second approach mentioned above, several authors have developed analytical equations for predicting the number of flushes required to move the deposited sediment bed (Bong et al. 2013; Chebbo et al. 1996). Likewise, the effects of pipe slope, bottom roughness, storage water level, and downstream water level, among others (Yang et al. 2019; Kuriqi et al. 2020) have also been studied in the past. As an example, Bong et al. (2013) proposed the following equation, where n_f is the number of flushes required to move the deposited sediment bed by 1 m:

$$n_f = 251.43y_s + 6.57 \quad (3)$$

In the third approach, several studies using ML and AI have been developed for predicting both bedload and suspended load transport in sewers, flumes, and streams. Several techniques as Artificial Neural Networks (Wan Mohtar et al. 2018; Bajirao et al. 2021), Random Forests (Khosravi et al. 2020; Safari 2020; Montes et al. 2021), and Vector Machines (Ebtehaj et al. 2017), among others, have been trained with experimental data collected at laboratory scale and tested with benchmark data found in the literature. These models outperform traditional regression formulas during the training stage but tend to underperform when applied to external datasets collected in sewers and flumes (Montes et al. 2021), i.e. during the testing stage.

Numerical studies mentioned above, based on the solution of the Saint-Venant and Exner coupled-equations for sediment transport under unsteady flow conditions, show similar predictions of the sediment thickness changes compared to the experimental data collected, i.e. the models show good accuracy prediction. Despite the solutions and simulations based on Saint Venant-Exner equations showing good accuracy, in practice, the application for operational and management practices is complex and non-pragmatic. Also, the analytical and dimensionless equations proposed by Bong et al. (2013) and Yang et al. (2019), do not include important parameters such as the pipe/flume geometry and the sediment characteristics. Finally, AI and ML models are largely black-box models (Montes et al. 2021), limiting their interpretability for practical applications.

The above gaps are addressed here by developing a new parsimonious regression-based model using the Evolutionary Polynomial Regression – Multi-Objective Genetic Algorithm (EPR-MOGA) (Giustolisi and Savic, 2009) strategy. EPR-MOGA is a data-driven method which combines genetic algorithm with evolutionary computing for finding polynomial structures. Due to its characteristics, the returned symbolic

expressions can be compared with existing models in terms of the input variables, exponent coefficients, and technical insight on the phenomenon (Montes et al. 2020a) while reducing the risk of overfitting.

This paper aims to propose a new model for predicting the sediment transport rate during flushing operations in sewers. The novelty of this model is the inclusion of flushing “dam break” hydrograph, pipe geometry, and deposited sediment characteristics in a simple polynomial expression. The new model developed here can be used to optimize flushing schemes and reduce the volume of water required for cleaning sewers.

2. EXPERIMENTAL METHODS AND DATA COLLECTION

The collection of experimental data was carried out in two pipes with diameters of 209 mm and 595 mm (Montes et al. 2020b), both located at the Hydraulics Laboratory of the University of the Andes, Colombia. A sediment bed with a near-uniform thickness and width was prepared at the bottom of the pipes, using uniformly graded sediment material ranging from 0.21 mm to 2.6 mm. These particles had a specific gravity between 2.57 and 2.67, which was calculated using the pycnometer method (ASTM D854-14, 2014). The experiments were carried out under unsteady flow conditions, simulating the “dam break” waves produced during a flushing event. The methodology used for data collection and further details of both experimental setups are described below.

2.1. 209 mm pipe setup

The 209 mm diameter acrylic pipe had a length of 10.58 m and was supported on six hydraulic jacks, which allowed to vary the pipe slope between 0.64% and 1.20%. This pipe was connected to a 200 mm solenoid valve, which controlled the inflow into the setup from a 3.5 m³ upstream tank. A downstream tank with a V-Notch weir was used to

measure the water discharge. A real-time water level sensor was used to measure the water height over the weir to calculate the water discharge rate using the V-Notch equation. The calculated discharge was also checked using an ABB- Electromagnetic flowmeter sensor installed upstream of the pipe. Two additional real-time water level sensors were installed along the pipe, aiming to measure the stage hydrograph produced by the flushing waves. Figure 1 shows the general scheme of the experimental setup.

The experimental data was collected as follows. Firstly, the solenoid valve was fully opened, allowing a base flowrate ranging from 0.002 l s^{-1} to 0.414 l s^{-1} . The opening of this valve simulates the ‘dam break hydrograph’ produced during a flushing operation in a real sewer pipe (e.g. using a Hydrass or a Hydrosel self flushing gate). Secondly, a sediment bed with near-uniform thickness and width was located at the bottom of the pipe. At this point, the base flowrate helped the formation of the deposited bed along a 3.3 m section. Thirdly, the solenoid valve was completely closed for storing a volume of water between 0.10 m^3 and 0.31 m^3 in the upstream tank. Fourthly, the solenoid valve was opened between 60% and 100% and the opening time was set to 15 sec for all tests. When the first discharged wave reached the sediment bed, the movement of the bed was tracked over time. The sediment velocity (V_s) was calculated using the values of the time and deposited bed displacement during the peak flow. The above procedure was repeated for different accumulated upstream water volume and percentage of the solenoid valve opening.

[Figure 1 near here]

2.2. 595 mm pipe setup

The pipe was 10.5 m long and supported on a mechanical steel truss, which allowed to modify the slope in a range between 0.04% and 3.44%. The base flow for the experiments,

ranging from 1.03 l s^{-1} to 9.98 l s^{-1} , was provided by a 40 BHP pump that supplied water to a 30 m^3 upstream storage which was directly connected to the pipe. For evaluating unsteady flow conditions in this pipe, a second 10 BHP submersible pump was located inside the downstream tank. This pump was directly connected to the upstream tank and was controlled with a variable frequency drive programmed before the experiment to create a pulse with a maximum peak flow of 30 l s^{-1} . Three water level sensors were used to record water depths in the experimental setup. Two of them were installed in the pipe to collect the stage hydrograph, and one was installed in the upstream tank. Full details of the experimental setup were described in Montes et al. (2020b) and are shown in Figure 2.

[Figure 2 near here]

For this setup, the data was collected as follows. Firstly, the pipe slope was adjusted using the mechanical steel truss and measured with a dumpy level. Secondly, the flow control valve on the upstream tank was opened to supply a base flow to the pipe. Thirdly, a deposited sediment bed with a near-uniform width was prepared at the bottom of the pipe over a minimum length of 1.5 m. At this point, to compare the flushing efficiency under similar conditions, the maximum sediment bed velocity was verified as 0.03 m s^{-1} . If this condition was not fulfilled, the pipe slope or the base flow were changed. Fourthly, the submersible pump, with its variable frequency drive, was activated to simulate the ‘dam break hydrograph’, which is similar to those produced by the flushing gates in real sewers. The water levels were recorded each 0.025 sec and the position of the sediment bed was tracked. The sediment velocity was calculated using the same procedure followed on the acrylic setup.

2.3. Experimental data collected

Using the experimental rig and approach described above, a total of 57 and 64 experiments were carried out in the 209 mm acrylic pipe and 595 mm PVC pipe, respectively. Several variables related to the pipe geometry, sediment properties, and flushing hydraulics, including the base time (t_b), peak time (t_p), base flow (Q_b), and peak flow (Q_p) were recorded in each experiment, as shown in Figure 3. The experimental data collected in both acrylic and PVC pipes are presented in Table 1, where S_o is the pipe slope, D the pipe diameter, Y the water level in the pipe, R the hydraulic radius, d the mean particle diameter, SG the specific gravity, y_s the sediment thickness, V_f the water velocity, and V_s the sediment velocity.

[Figure 3 near here]

[Table 1 near here]

A flushing discharge hydrograph and a plot showing the sediment bed position related with each run are presented in Table 1. The shape and magnitude of the hydrograph are directly related to the sediment bed velocity, and consequently, the sediment bed position. As an example, for six runs, the variation in the sediment bed position and hydrograph characteristics, in both acrylic and PVC pipe, are presented in Figure 4. Full details of each run shown in Figure 4 are presented in Table 1.

[Figure 4 near here]

Figure 4A and Figure 4B show the relation between the flushing discharge hydrograph and the sediment bed position for tests conducted on the acrylic pipe. As seen in these figures, particle size is a more important variable in defining the sediment position, compared to the peak flow in the hydrograph. Even though the run 82 considers

a higher peak flow ($Q_p = 5.55 \text{ l s}^{-1}$), the final position of the sediment bed ($= 0.41 \text{ m}$) is lower than the run 96 ($= 2.62 \text{ m}$) when the peak flow is lower ($Q_p = 2.08 \text{ l s}^{-1}$). This occurs because the particle diameter is more relevant compared to the peak flow.

Figure 4C and Figure 4D show the relation between the flushing discharge hydrograph and the sediment bed position for tests in 595 mm setup. The relationship between the discharge hydrograph and the sediment bed position is proportional. For run no. 36 and 61, the mean particle diameter was 2.60 mm, but the pipe slope was 1.65% and 1.82%, respectively. Figure 4D shows that maintaining the mean particle diameter constant as the pipe slope increases, the final bed position increases.

3. MODEL DEVELOPMENT

3.1. Graphical analysis

A graphical analysis was developed to visualize the relationships between the variables collected in each experiment. The relationship between sediment velocity and flow velocity (V_s/V_f) was plotted against other dimensionless parameters, as shown in Figure 5. These dimensionless parameters have been previously identified as relevant for predicting sediment transport in sewer pipes in previous literature (Ab Ghani and Azamathulla, 2011; Ebtehaj and Bonakdari, 2016; May et al. 1996; Kuriqi et al. 2020; Montes et al. 2021). Two of these parameters include the dimensionless grain size (d/R) and the Shields parameter (ψ), defined in Eq. (4):

$$\psi = \frac{RS_o}{(SG - 1)d} \quad (4)$$

Based on the results shown in Figure 5, the following observations can be made:

- In general, higher values of the Shields parameter lead to higher values of V_s/V_f . This can be clearly seen in the acrylic pipe (Figure 5a) because of the constant slope value adopted in the experimental rig. Furthermore, high values of S_o and R lead to higher sediment velocities due to higher critical shearing stress (i.e. the applied forces are higher than the submerged weight of the particle). In contrast, deposited materials with high density of particle diameters result in lower sediment velocities.
- The direct relationship between V_s/V_f and the Shields parameter coincides with the inversely proportional relationship between V_s/V_f and d/R , shown in Figure 5c and Figure 5d. This is observed because the Shields parameter includes the ratio R/d , as shown in Eq. (4).
- Figure 5e shows the inversely proportional relationship between V_s/V_f and the dimensionless parameter Q_b/Q_p , meaning that higher and steeper discharge hydrographs (i.e. lower ratios Q_b/Q_p) show higher V_s/V_f values.
- In general, based on what was previously mentioned, higher values of S_o and R and lower values of d , SG , and Q_b/Q_p lead to higher sediment velocities V_s .

[Figure 5 near here]

3.2. Evolutionary Polynomial Regression model

A new regression-based model was developed here to predict the dimensionless ratio V_s/V_f during flushing operation. The new model includes the group of parameters identified in previous studies (Ab Ghani and Azamathulla, 2011; Ebtehaj and Bonakdari, 2016; May et al. 1996; Montes et al. 2021) and the graphic analysis carried out for the experimentally collected data, as shown in Figure 5.

Evolutionary polynomial regression (EPR) is a hybrid regression technique that combines numerical and symbolic regression (Giustolisi and Savic, 2006, 2004). In its original formulation, it used single objective genetic algorithms to explore the formula space, and then it estimates the least-squares regression coefficients. This technique has proved to be effective when the number of polynomial terms is not large (Giustolisi and Savic, 2009). To solve these issues, Giustolisi and Savic (Giustolisi and Savic, 2009) introduced the EPR technique combined with a Multi-Objective Genetic Algorithm (MOGA). This novel technique maximises the model accuracy (i.e. minimises the sum of squared errors) and minimises the number of polynomial coefficients, and therefore improves the exploration of the space of symbolic formulas. EPR-MOGA considers some pseudo-polynomial expressions such as (Giustolisi and Savic, 2009):

$$\hat{\mathbf{Y}} = a_0 + \sum_{j=1}^m a_j (\mathbf{X}_1)^{ES(j,1)} \cdot \dots \cdot (\mathbf{X}_k)^{ES(j,k)} \cdot f((\mathbf{X}_1)^{ES(j,k+1)}) \cdot \dots \cdot f((\mathbf{X}_k)^{ES(j,2k)}) \quad (5)$$

where $\hat{\mathbf{Y}}$ is the vector of model predictions; ES and j the matrix of candidate exponents and the inner function, respectively, both selected by the user; m the number of terms; a_0 the bias term; a_j the adjustable parameters estimated by linear least squares and \mathbf{X}_j the candidate explanatory variables. The inner function f defined by the user can be logarithmic, exponential, tangent hyperbolic, or secant hyperbolic, and must be selected according to the physics of the problem studied. The EPR technique returns a range of models showing the influence of different explanatory factors by progressively adding these as input variables to monomial formulas, starting from the most important ones. For each EPR identified model, the following performance indices are calculated: the Bayesian Information Criterion (BIC) and the Coefficient of Determination (R^2), as shown in Eq. (6) and Eq. (7), respectively.

$$BIC = \left(1 + d \frac{\log(n)}{n}\right) \left(\sum_{i=1}^n (Y^* - Y)^2\right) \quad (6)$$

$$R^2 = 1 - \frac{\sum_{i=1}^n (Y^* - Y)^2}{\sum_{i=1}^n (Y^* - \bar{Y}^*)^2} \quad (7)$$

where Y^* and Y are the observed and calculated data, respectively, n is the number of data, d the number of parameters included in the model and \bar{Y}^* the mean of observed data. The Coefficient of Determination measures the fraction of variance that can be explained. Note that this coefficient varies between 0 and 1, where 1 denotes a perfect match between observed and calculated data. The Bayesian Information Criterion measures the trade-off between accuracy and parsimony of the model. This measure penalises formulas with large number of parameters. The model with the lowest BIC value is selected as optimal.

The new model was constructed to predict the dimensionless relation V_s/V_f , i.e. the vector of model predictions \hat{Y} is defined as V_s/V_f . The matrix of candidate exponents was defined with values ranging from -2.50 to 2.50, considering steps of 0.1, i.e. $ES = [-2.50, -1.40, \dots, 1.40, 2.50]$. The matrix of candidate explanatory variables is defined as follows:

$$\mathbf{X}_j = \left[\psi, \frac{d}{R}, \frac{Q_b}{Q_p}, \frac{y_s}{R}, \frac{t_b}{t_p}, \beta \right] \quad (8)$$

Using previous considerations, and randomly splitting the experimental data collected on the 209 mm and 595 mm pipes, for both training (75% of the data) and testing (25% of the data) stages, the results shown in Table 2 were obtained using the EPR-MOGA strategy.

[Table 2 near here]

Table 2 shows the Pareto front (i.e. range of models) generated by the EPR, together with the corresponding BIC and R^2 values. For example, the best 1 input variable model includes only the Shields parameter as an explanatory variable for predicting the V_s/V_f ($V_s/V_f = 0.17\psi^{0.5}$). This is the least complex, i.e. most parsimonious model hence, unsurprisingly, it has a rather low prediction accuracy ($BIC = -48.21$ and $R^2 = 0.38$). In contrast, the 6-variable model includes all candidate explanatory factors $\left(V_s/V_f = 2.48\psi^{1.4} \left(\frac{Q_b}{Q_p}\right)^{-0.3} \left(\frac{d}{R}\right)^{0.9} \left(\frac{y_s}{R}\right)^{0.1} \left(\frac{t_b}{t_p}\right)^{-0.2} \beta\right)$, resulting in low parsimony model but with improved prediction accuracy ($BIC = -92.22$ and $R^2 = 0.64$). Based on this, the model that shows the best trade-off between accuracy and parsimony is the model with 3 input variables. This model is shown in Eq. (9).

$$\frac{V_s}{V_f} = 8.13 \left(\frac{d}{R}\right)^{0.90} \left(\frac{RS_o}{(SG-1)d}\right)^{1.40} \left(\frac{Q_b}{Q_p}\right)^{-0.30} \quad (9)$$

Or rearranging the above formula to simplify the d/R term:

$$\frac{V_s}{V_f} = 8.13 \left(\frac{d}{R}\right)^{-0.50} \left(\frac{S_o}{(SG-1)}\right)^{1.40} \left(\frac{Q_b}{Q_p}\right)^{-0.30} \quad (10)$$

The obtained model was used to estimate the flushing efficiency in larger pipes considering different flow conditions and sediment characteristics. Further details are described in the section below. The model's accuracy can be seen in Figure 6 for both training and testing datasets.

[Figure 6 near here]

As it can be seen from the above equation and figure, Eq. (10) is consistent with the graphical analysis presented in Figure 6. Further, it can be seen from the model obtained that $\frac{S_o}{(SG-1)}$ is the most important feature for predicting the sediment velocity

during the flushing cleaning operation - the more the pipe slope increases, the higher the particle velocity is (note that the $\frac{S_o}{(SG-1)}$ parameter comes from the Shields parameter). The Shields parameter shows the ratio between the hydrodynamic forces acting on the particles and the resistance due to gravity. This parameter has been identified as one of the most relevant for predicting the incipient motion in sewers (Delleur, 2001; Safari et al. 2018; Wan Mohtar et al. 2018). As mentioned above, V_s/V_f is inversely proportional to d/R , which is consistent with the results shown by EPR-MOGA model.

4. RESULTS AND DISCUSSION

The new model shown in Eq. (10) was used to generate charts to estimate flushing efficiency as a function of the characteristics of the discharged hydrograph, the pipe geometry and the sediment properties. In this context, two flushing-efficiency measures were defined as a function of the area of deposited bed (A_s) and the sediment velocity. The first measure, Q_s , is the volume of sediment removed by unit time (i.e. the sediment flow rate = $A_s V_s$). The second measure, t_e , is the flushing time required to clean 1.0 m of the pipe ($= 1/V_s$). Figure 7 and Figure 8 were constructed for several pipe diameters using previous measures. To construct these figures, the less-significant variables identified by the EPR-MOGA model (as shown in Table 2) remained constant. The sediment thickness was defined as $y_s/D = 1\%$, the specific gravity of the sediments as 2.6, and the relation between the base and peak time of the hydrograph as $t_b/t_p = 5.0$.

[Figure 7 near here]

The following observations can be made from Figure 7 and Figure 8:

- Q_s is inversely proportional to d and Q_b/Q_p . In addition, Q_s seems to be near-steady for particle diameters greater than 1.5 mm in pipes with diameters less than

800 mm. All above for the same pipe slope and Q_b/Q_p relation. Increasing the pipe slope directly increase the sediment transport rate.

- As the Q_b/Q_p ratio increases, the sediment removal rate decreases. For example, in Figure 7a, when $Q_b/Q_p = 0.25$ in a 1200 mm diameter pipe containing a deposited sediment bed with $d = 1$ mm, $Q_s = 0.5 \times 10^{-4}$ m³/s, while for $Q_b/Q_p = 0.75$ the Q_s value changes to 0.2×10^{-4} m³/s, that is 60% less (as shown in Figure 7c).
- Flushing discharges seem to be more efficient in larger sewer pipes. The sediment transport rate can be five times higher in 2000 mm diameter pipes, compared to 1200 mm diameter pipes.
- Figure 8 shows a direct relationship between t_e and d and Q_b/Q_p . Based on this, as d increases and Q_p decreases, the required flushing time to clean 1 meter of the pipe increases. For example, in Figure 8d when $Q_b/Q_p = 0.25$ in a 800 mm diameter pipe containing a deposited sediment bed with $d = 1.5$ mm, $t_e = 20$ sec, while for $Q_b/Q_p = 0.75$ the t_e value changes to 45 sec, that is 125% more (as shown in Figure 8f)
- The flushing time decreases as the S_o and D increase. That is, flushing is a more efficient technique in large and steep pipes.

[Figure 8 near here]

4.1. Model comparison

To test the accuracy of the model shown in Eq. (10), the case study described in Laplace et al. (2003) was used. This case study is located in Marseille, France, on a combined sewer network. Specifically, this study considers an ovoid section of 1700 mm, 120 m long with a bottom slope of 0.03%. A near-uniform deposited bed of 140 mm thickness

was observed along the entire length of the flume. The deposited bed was characterised as coarser upstream ($d = 8$ mm) and finer downstream ($d = 0.6$ mm). Full details are shown in Laplace et al. (2003).

Using a Hydrass-flushing gate located inside the section, a series of flushes were conducted for testing the efficiency on removing the deposited material. During each flush, a total volume of 6.0 m^3 of water was discharged into the pipe. As reported by Laplace et al. (2003), the mass of particles eroded during the first flush was 6.3 kg , i.e. the removal rate was 1.08 kg of material per 1.0 m^3 of water ($= 1.08 \text{ kg m}^{-3}$).

Two existing procedures are compared with the new EPR-MOGA model presented in Eq. (10): the model proposed by Bong et al. (2013) (i.e. Eq. (3)) and the design tables shown by Dettmar (2007). To compare the results, several initial conditions are defined based on the case study description, which are outlined as follows:

- (1) Thickness of the deposited bed (y_s) = 0.14 m
- (2) Peak flow during flushing operation (Q_p) = 100 l s^{-1}
- (3) Specific gravity of the sediments (SG) = 2.60
- (4) Mean particle diameter (d) = $0.6 - 8.0 \text{ mm}$
- (5) Mass of material per meter of pipe = 54.22 kg m^{-1}

According to Bong et al. (2013), the number of flushes required to move 1 m of deposited material can be estimated by applying Eq. (3). For this equation, the number of flushes is only a function of the thickness of the deposited bed. As a result, 42 flushes ($= 250.6 \text{ m}^3$ of water) can potentially remove 54.22 kg of the deposited material (i.e. the removal rate is 0.21 kg m^{-3}). Design tables proposed by Dettmar (2007) suggest a flushing

volume of 48 m³ for a basic cleaning of the 150 m long sewer (i.e. a full removing of the deposited material). No removal rates are provided by Dettmar (2007).

Finally, using the new model proposed in this study, a range of removal rates are obtained as a function of the mean particle diameter. Potentially, a flushing volume of 10.18 m³ can remove 14.5 kg of deposited material with a mean particle diameter of 0.6 mm (i.e. the removal rate is 0.40 kg m⁻³). By changing the particle size of the deposited material to 8.3 mm, the removal rate is 1.25 kg m⁻³.

[Table 3 near here]

As shown in Table 3, a direct comparison of the method proposed by Dettmar (2007) and the results reported by Laplace et al. (2003) is not possible. However, this method seems to underestimate the real volume required to remove the deposited bed. Relevant parameters such as the mean particle diameter and the sewer hydraulics are not included in this method. Due to the pipe slope in the case of study is almost flat, obtaining minimum shear stress of 5.0 N m⁻² for cleaning the pipe, according to Dettmar (2007), requires larger flows.

The model presented by Bong et al. (2013) is a good approach for determining the number of flushes required to move the deposited material. However, because of the non-inclusion of relevant pipe hydraulics and sediment parameters, the results are underestimated, compared to the values reported by Laplace et al. (2003).

4.2. Model considerations

The new model presented here shows good prediction accuracy with the data reported by Laplace et al. (2003). This is explained by the inclusion of relevant parameters for predicting the removal rate during the flushing operation. The model also shows good

extrapolation capabilities under different sewer diameters and a wide range of variations of the mean particle diameter.

The Shields parameter was selected as the most important one due to the highest value in the regression coefficient and the Pareto solution provided by the EPR-MOGA strategy. This was expected since this parameter determines the threshold condition of sediment initiation motion. The sediment thickness parameter is less important for defining the sediment velocity during the flushing operation due to the low regression coefficient presented in Table 2. As a result, the model can be used in both combined and storm sewers, where the sediment thickness ranges from 10 mm to 100 mm and 10 mm to 330 mm, respectively (Bong et al. 2016).

The model includes the peak flow as an explanatory variable for predicting sediment transport rate. Higher peak flow implies a higher removal rate since higher shear stresses are generated at the bottom of the pipe. The observed shear stress values (ranging from 2.0 N/m^2 to 6.5 N/m^2 in the PVC pipe) are consistent with those reported in the literature for the erosion and transport of bed material (Dettmar, 2007; Campisano et al. 2008; Yang et al. 2019). However, since the model only considers transport as bedload, some fine particles may be eroded and transported in suspension (which has been identified as one of the major sources of pollution in CSO (Laplace et al. 2003; Saul et al. 2003)), due to the high turbulence of the flow. This is particularly important in well-graded materials where wide ranges of mean particle sizes are present.

Even though the new model was developed considering a wide range of variations in input variables, some limitations exist. The granular material used in the experiments cannot represent the cohesive properties of sediments found in real sewer systems. As a result, an increased bed resistance to erosion can be seen in practice (Campisano et al.

2019). In addition, the lowest pipe slope value considered during the tests was 0.644%, which is higher than the minimum self-cleansing value recommended in several industry design codes and water utilities design manuals (e.g. Health Research Inc. (2004), as quoted by Montes et al. (2019)).

5. CONCLUSIONS

This study proposes a simple model to predict the sediment transport rate in practice based on data collected from a set of 121 lab experiments conducted on a 209 mm diameter acrylic pipe and 595 mm diameter PVC pipe. The data collected this way were processed using the EPR-MOGA modelling technique. A new model for predicting the sediment velocity during flushing operation was developed and used for constructing design charts. Based on the results obtained, the following conclusions are made:

- (1) The new model developed and presented here can predict the sediment transport rate during flushing discharges accurately in practice. This model includes the group of parameters that most affect the flushing efficiency in sewer pipes.
- (2) The sediment transport rate is principally affected by four parameters: pipe slope, pipe diameter, particle diameter and discharged peak flow. In pipes with large diameters and slopes, the flushing is more effective. This is because of the high regression exponents for both $\frac{S_o}{(SG-)}$ and d/R variables obtained in the EPR-MOGA model presented here. The sediment transport is not significantly affected by the value of the deposited sediment thickness.
- (3) The new model proposed outperforms the simplified models and methods reported in the literature in terms of removal sediment rate prediction. This is seen by the better prediction accuracy shown when compared to the case study reported by Laplace et al. (2003).

(4) Existing models such as Bong et al. (2013) and Dettmar (2007) for predicting sediment transport tend to underestimate the total volume of water required to clean a deposited sediment bed. The EPR-MOGA model is more accurate in predicting the sediment transport rate as this model includes parameters affecting the flushing efficiency, such as flushing hydraulics, pipe geometry and sediment properties.

Based on the conclusions mentioned above, the new flushing model can be useful for designing flushing schemes during the operational stage of existing sewer pipes in engineering practice. Further research is recommended to test the model proposed in real sewer pipes under different sediment (i.e. cohesive materials) and hydraulic conditions.

Acknowledgements

The authors would like to thank Professor Orazio Giustolisi who developed and made available for free the EPR software used in this research.

Disclosure Statement

No potential conflict of interest was reported by the author(s).

Funding

This research received no external funding.

REFERENCES

- Ab Ghani, A., and Azamathulla, H. 2011. "Gene-Expression Programming for Sediment Transport in Sewer Pipe Systems." *Journal of Pipeline Systems Engineering and Practice* 2(3): 102–106. [https://doi.org/10.1061/\(ASCE\)PS.1949-1204.0000076](https://doi.org/10.1061/(ASCE)PS.1949-1204.0000076)
- Ashley, R., Bertrand-Krajewski, J., Hvitved-Jacobsen, T., and Verbanck, M., 2004. *Solids in Sewers: Characteristics, Effects and Control of Sewer Solids and Associated Pollutants*. London: IWA Publishing. <https://doi.org/10.2166/9781780402727>
- ASTM D854-14, 2014. *Standard Test Methods for Specific Gravity of Soil Solids by*

492 *Water Pycnometer*. West Conshohocken, PA: ASTM International.

493 Azamathulla, H., Ab Ghani, A., and Fei, S., 2012. "ANFIS-based approach for predicting
494 sediment transport in clean sewer." *Applied Soft Computing Journal* 12(3): 1227–
495 1230. <https://doi.org/10.1016/j.asoc.2011.12.003>

496 Bajirao, T., Kumar, P., Kumar, M., Elbeltagi, A., and Kuriqi, A. 2021. "Superiority of
497 Hybrid Soft Computing Models in Daily Suspended Sediment Estimation in Highly
498 Dynamic Rivers." *Sustainability* 13(2): 542. <https://doi.org/10.3390/su13020542>

499 Bertrand-Krajewski, J., Bardin, J., Gibello, C., and Laplace, D. 2003. "Hydraulics of a
500 sewer flushing gate." *Water Science and Technology* 47(4), 129–136.
501 <https://doi.org/10.2166/wst.2003.0237>

502 Bong, C., Lau, T., and Ab Ghani, A. 2016. "Potential of tipping flush gate for
503 sedimentation management in open stormwater sewer." *Urban Water Journal* 13(5):
504 486–498. <https://doi.org/10.1080/1573062X.2014.994002>

505 Bong, C., Lau, T., Ab Ghani, A., and Chan, N. "Sediment deposit thickness and its effect
506 on critical velocity for incipient motion." *Water Science and Technology* 74(8):
507 1876-1884. <https://doi.org/10.2166/wst.2016.376>

508 Bong, C., Lau, T., and Ab Ghani, A. 2013. "Hydraulics characteristics of tipping sediment
509 flushing gate." *Water Science and Technology* 68(11): 2397–2406.
510 <https://doi.org/10.2166/wst.2013.498>

511 British Standard Institution, 2014. *Management and Control of Operational Activities in*
512 *Drain and Sewer Systems Outside Buildings. Part 1: Cleaning*. London, UK.

513 Campisano, A., Creaco, E., and Modica, C. 2008. "Laboratory investigation on the effects
514 of flushes on cohesive sediment beds." *Urban Water Journal* 5(1): 3–14.
515 <https://doi.org/10.1080/15730620701726259>

516 Campisano, A., Creaco, E., and Modica, C. 2007. "Dimensionless Approach for the
517 Design of Flushing Gates in Sewer Channels." *Journal of Hydraulic Engineering*
518 133(8): 964–972. [https://doi.org/10.1061/\(ASCE\)0733-9429\(2007\)133:8\(964\)](https://doi.org/10.1061/(ASCE)0733-9429(2007)133:8(964))

519 Campisano, A., Creaco, E., and Modica, C. 2006. "Experimental analysis of the hydrass
520 flushing gate and laboratory validation of flush propagation modelling." *Water*
521 *Science and Technology* 54(6-7): 101–108. <https://doi.org/10.2166/wst.2006.608>

522 Campisano, A., Creaco, E., and Modica, C. 2004. "Experimental and numerical analysis
523 of the scouring effects of flushing waves on sediment deposits." *Journal of*
524 *Hydrology* 299(3-4): 324–334. <https://doi.org/10.1016/j.jhydrol.2004.08.009>

525 Campisano, A., and Modica, C. 2003. "Flow velocities and shear stresses during flushing
526 operations in sewer collectors." *Water Science and Technology* 47(4): 123–128.
527 <https://doi.org/10.2166/wst.2003.0236>

528 Campisano, A., Modica, C., Creaco, E., and Shahsavari, G. 2019. "A model for non-
529 uniform sediment transport induced by flushing in sewer channels." *Water Research*
530 163: 114903. <https://doi.org/10.1016/j.watres.2019.114903>

- 531 Caviedes-Voullième, D., Morales-Hernández, M., Juez, C., Lacasta, A., and García-
 532 Navarro, P. 2017. "Two-dimensional numerical simulation of bed-load transport of
 533 a finite-depth sediment layer: Applications to channel flushing." *Journal of*
 534 *Hydraulic Engineering* 143(9):04017034.
 535 [https://doi.org/10.1061/\(ASCE\)HY.1943-7900.0001337](https://doi.org/10.1061/(ASCE)HY.1943-7900.0001337)
- 536 Chebbo, G., Laplace, D., Bachoc, A., Sanchez, Y., and Le Guennec, B. 1996. "Technical
 537 solutions envisaged in managing solids in combined sewer networks." *Water*
 538 *Science and Technology* 33(9): 237–244. [https://doi.org/10.1016/0273-](https://doi.org/10.1016/0273-1223(96)00392-7)
 539 [1223\(96\)00392-7](https://doi.org/10.1016/0273-1223(96)00392-7)
- 540 Creaco, E., and Bertrand-Krajewski, J. 2009. "Numerical Simulation of flushing effect
 541 on sewer sediments and comparison of Four sediment transport formulas." *Journal*
 542 *of Hydraulic Research* 47(2): 195–202. <https://doi.org/10.3826/jhr.2009.3363>
- 543 De Sutter, R., Huygens, M., and Verhoeven, R. 1999. "Unsteady flow sediment transport
 544 in a sewer model." *Water Science and Technology* 39(9): 121–128.
 545 [https://doi.org/10.1016/S0273-1223\(99\)00224-3](https://doi.org/10.1016/S0273-1223(99)00224-3)
- 546 Delleur, J. 2001. "New results and research needs on sediment movement in urban
 547 drainage." *Journal of Water Resources Planning and Management* 127(3): 186-193.
 548 [https://doi.org/10.1061/\(ASCE\)0733-9496\(2001\)127:3\(186\)](https://doi.org/10.1061/(ASCE)0733-9496(2001)127:3(186))
- 549 Dettmar, J. 2007. "A new planning procedure for sewer flushing." Paper presented at the
 550 NOVATECH 2007 – Sixth International Conference on Sustainable Techniques and
 551 Strategies in Urban Water Management, Lyon, June 25-28.
- 552 Dettmar, J. 2005. "Beitrag zur Verbesserung der Reinigung von Abwasserkanälen." PhD
 553 diss., RWTH Aachen University.
- 554 Dettmar, J., Rietsch, B., and Lorenz, U. 2002. "Performance and Operation of Flushing
 555 Devices - Results of a Field and Laboratory Study." *Global Solutions for Urban*
 556 *Drainage: Proceedings of the Ninth International Conference on Urban Drainage:*
 557 1–10. [https://doi.org/10.1061/40644\(2002\)291](https://doi.org/10.1061/40644(2002)291)
- 558 Ebtehaj, I., and Bonakdari, H. 2016. "Bed Load Sediment Transport in Sewers at Limit
 559 of Deposition." *Scientia Iranica* 23(3): 907–917.
 560 <https://doi.org/10.24200/sci.2016.2169>
- 561 Ebtehaj, I., Bonakdari, H., Shamshirband, S., Ismail, Z., and Hashim, R. 2017. "New
 562 approach to estimate velocity at limit of deposition in storm sewers using vector
 563 machine coupled with firefly algorithm." *Journal of Pipeline Systems Engineering*
 564 *and Practice* 8(2): 04016018.
 565 [https://doi.org/10.1061/\(ASCE\)PS.1949-1204.0000252](https://doi.org/10.1061/(ASCE)PS.1949-1204.0000252)
- 566 Fan, C. 2004. *Sewer Sediment and Control A Management Practices Reference Guide*.
 567 U.S. Environmental Protection Agency, Washington, DC, EPA/600/R-04/059.
- 568 Fan, C., Field, R., Pisano, W., Barsanti, J., Joyce, J., and Sorenson, H. 2001. "Sewer and
 569 Tank Flushing for Sediment, Corrosion, and Pollution Control." *Journal of Water*
 570 *Resources Planning and Management* 127(3): 194–201.

571 [https://doi.org/10.1061/\(ASCE\)0733-9496\(2001\)127:3\(194\)](https://doi.org/10.1061/(ASCE)0733-9496(2001)127:3(194))

572 Giustolisi, O., and Savic, D. 2009. “Advances in data-driven analyses and modelling
573 using EPR-MOGA.” *Journal of Hydroinformatics* 11(3-4): 225–236.
574 <https://doi.org/10.2166/hydro.2009.017>

575 Giustolisi, O., and Savic, D. 2006. “A symbolic data-driven technique based on
576 evolutionary polynomial regression.” *Journal of Hydroinformatics* 8(4): 207–222.
577 <https://doi.org/10.2166/hydro.2006.020>

578 Giustolisi, O., and Savic, D. 2004. “A Novel Genetic Programming Strategy:
579 Evolutionary Polynomial Regression.” *Proceedings of the 6th International
580 Conference on Hydroinformatics*: 787–794.
581 https://doi.org/10.1142/9789812702838_0097

582 Guo, Q., Fan, C., Raghaven, R., and Field, R. 2004. “Gate and Vacuum Flushing of Sewer
583 Sediment: Laboratory Testing.” *Journal of Hydraulic Engineering* 130(5): 463–
584 466. [https://doi.org/10.1061/\(ASCE\)0733-9429\(2004\)130:5\(463\)](https://doi.org/10.1061/(ASCE)0733-9429(2004)130:5(463))

585 Health Research Inc. (2004). “Recommended standards for wastewater facilities.” *A
586 Report of the Wastewater Committee* 12224(518): 1–102.

587 Hlavinek, P., Malanik, S., Raclavsky, J., Sulcova, V., Montero, C., and Villanueva, A.
588 2005. *WP4 Deliverable 11: Survey of Operational Options*. Brno.

589 Khosravi, K., Cooper, J., Daggupati, P., Thai Pham, B., and Tien Bui, D. 2020. “Bedload
590 transport rate prediction: Application of novel hybrid data mining techniques”
591 *Journal of Hydrology* 585: 124774 <https://doi.org/10.1016/j.jhydrol.2020.124774>

592 Kuriqui, A., Koçileri, G., and Ardiçlioğlu, M. 2020. “Potential of Meyer-Peter and Müller
593 approach for estimation of bed-load sediment transport under different hydraulic
594 regimes” *Modeling Earth Systems and Environment* 6: 129–137.
595 <https://doi.org/10.1007/s40808-019-00665-0>

596 Lainé, S., Phan, L., Malabat, D., and Duffros, B. 1998. “Flush Cleaning of Sewer Using
597 the Hydras-Valve.” Paper presented at the 4th International Conference on Urban
598 Drainage Modelling, London, September 21–24.

599 Laplace, D., Oms, C., Ahyerre, M., Chebbo, G., Lemasson, J., and Felouzis, L. 2003.
600 “Removal of the organic surface layer in combined sewer sediment using a flushing
601 gate.” *Water Science and Technology* 47(4): 19–26.
602 <https://doi.org/10.2166/wst.2003.0211>

603 May, R., Ackers, J., Butler, D., and John, S. 1996. “Development of design methodology
604 for self-cleansing sewers.” *Water Science and Technology* 33(9): 195–205.
605 [https://doi.org/10.1016/0273-1223\(96\)00387-3](https://doi.org/10.1016/0273-1223(96)00387-3)

606 Montes, C., Bohorquez, J., Borda, S., and Saldarriaga, J. 2019. “Impact of Self-Cleansing
607 Criteria Choice on the Optimal Design of Sewer Networks in South America.” *Water
608 (Switzerland)* 11(6): 1148. <https://doi.org/10.3390/w11061148>

609 Montes, C., Berardi, L., Kapelan, Z., and Saldarriaga, J. 2020a. “Predicting bedload

610 sediment transport of non-cohesive material in sewer pipes using evolutionary
611 polynomial regression – multi-objective genetic algorithm strategy.” *Urban Water*
612 *Journal* 17(2): 154-162. <https://doi.org/10.1080/1573062X.2020.1748210>

613 Montes, C., Vanegas, S., Kapelan, Z., Berardi, L., and Saldarriaga, J. 2020b. “Non-
614 deposition self-cleansing models for large sewer pipes.” *Water Science and*
615 *Technology* 81(3): 606–621. <https://doi.org/10.2166/wst.2020.154>

616 Montes, C., Kapelan, Z., and Saldarriaga, J. 2021. “Predicting non-deposition sediment
617 transport in sewer pipes using Random forest.” *Water Research* 189, 116639.
618 <https://doi.org/10.1016/j.watres.2020.116639>

619 NEIWPCC, 2003. Optimizing Operation, Maintenance, and Rehabilitation of Sanitary
620 Sewer Collection Systems. Lowell, MA.

621 Ristenpart, E. 1998. “Solids transport by flushing of combined sewers.” *Water Science*
622 *and Technology* 37(1): 171–178. [https://doi.org/10.1016/S0273-1223\(97\)00767-1](https://doi.org/10.1016/S0273-1223(97)00767-1)

623 Rodríguez, J., McIntyre, N., Díaz-Granados, M., and Maksimović, Č. 2012. “A database
624 and model to support proactive management of sediment-related sewer blockages.”
625 *Water Research* 46(15): 4571–4586. <https://doi.org/10.1016/j.watres.2012.06.037>

626 Safari, M. 2020. “Hybridization of multivariate adaptive regression splines and random
627 forest models with an empirical equation for sediment deposition prediction in open
628 channel flow.” *Journal of Hydrology* 590: 125392.
629 <https://doi.org/10.1016/j.jhydrol.2020.125392>

630 Safari, M., Mohammadi, M., and Ab Ghani, A. 2018. “Experimental studies of self-
631 cleansing drainage system design: A review.” *Journal of Pipeline Systems*
632 *Engineering and Practice* 9(4): 04018017. [https://doi.org/10.1061/\(ASCE\)PS.1949-1204.0000335](https://doi.org/10.1061/(ASCE)PS.1949-1204.0000335)

634 Sakakibara, T. 1996. “Sediments flushing experiment in a trunk sewer.” *Water Science*
635 *and Technology* 33(9): 229–235. [https://doi.org/10.1016/0273-1223\(96\)00391-5](https://doi.org/10.1016/0273-1223(96)00391-5)

636 Saul, A., Skipworth, P., Tait, S., and Rushforth, P. 2003. “Movement of Total Suspended
637 Solids in Combined Sewers.” *Journal of Hydraulic Engineering* 129(4): 298-307.
638 [https://doi.org/10.1061/\(ASCE\)0733-9429\(2003\)129:4\(298\)](https://doi.org/10.1061/(ASCE)0733-9429(2003)129:4(298))

639 Schaffner, J., and Steinhardt, J. 2006. “Numerical investigation of the self-acting flushing
640 system HydroFlush GS in Frankenberg/Germany.” Paper presented at the 2th
641 Conference on Sewer Operation and Maintenance, Vienna, October.

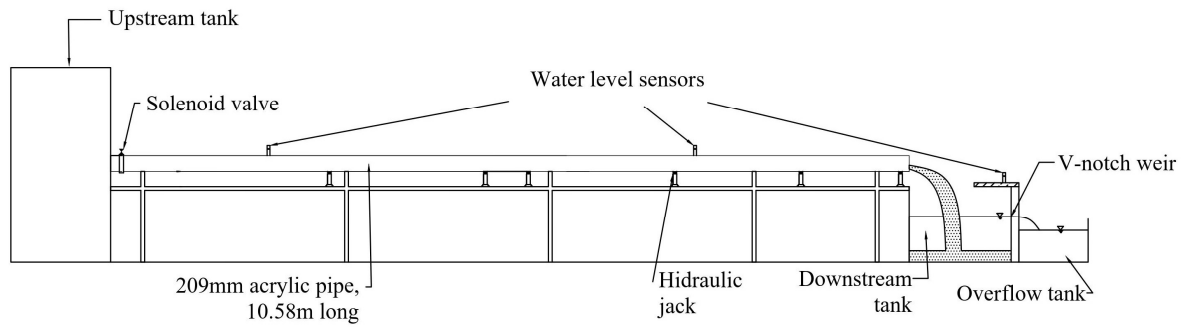
642 Shahsavari, G., Arnaud-Fassetta, G., and Campisano, A. 2017. “A field experiment to
643 evaluate the cleaning performance of sewer flushing on non-uniform sediment
644 deposits.” *Water Research* 118: 59–69 <https://doi.org/10.1016/j.watres.2017.04.026>

645 Shirazi, R., Campisano, A., Modica, C., and Willems, P. 2014. “Modelling the erosive
646 effects of sewer flushing using different sediment transport formulae.” *Water*
647 *Science and Technology* 69(6): 1198–1204. <https://doi.org/10.2166/wst.2013.810>

648 Wan Mohtar, W., Afan, H., El-Shafie, A., Bong, C., and Ab Ghani, A. 2018. “Influence

- 649 of bed deposit in the prediction of incipient sediment motion in sewers using
650 artificial neural networks.” *Urban Water Journal* 15(4): 296-302.
651 <https://doi.org/10.1080/1573062X.2018.1455880>
- 652 Yang, H., Zhu, D., Zhang, Y., and Zhou, Y. 2019. “Numerical investigation on bottom
653 shear stress induced by flushing gate for sewer cleaning.” *Water Science and*
654 *Technology* 80(2): 290–299. <https://doi.org/10.2166/wst.2019.269>
- 655 Yu, C., and Duan, J. 2014. “Two-Dimensional Finite Volume Model for Sediment
656 Transport in Unsteady Flow.” *World Environmental and Water Resources Congress*
657 *2014*: 1432–1441. <https://doi.org/10.1061/9780784413548.144>

658



659

660

661

Figure 1. Experimental setup used to collect the unsteady flow data in the 209 mm acrylic pipe.

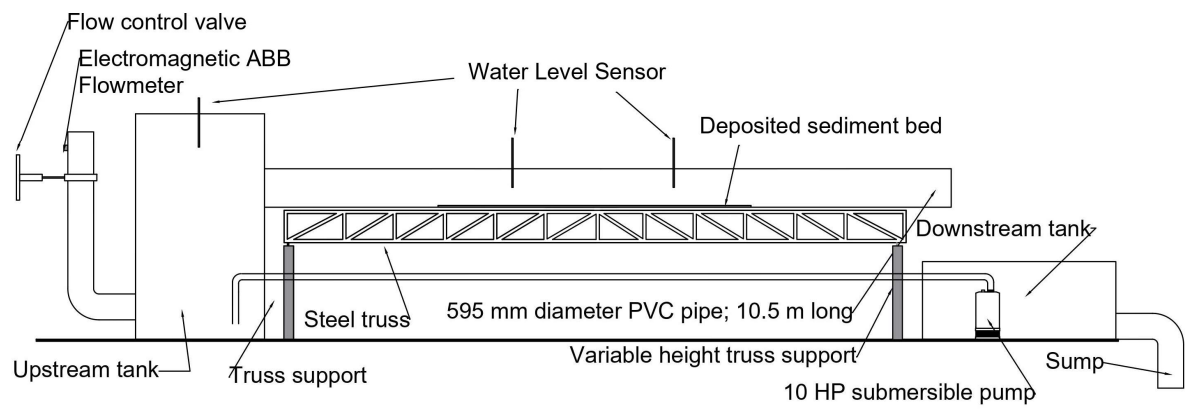
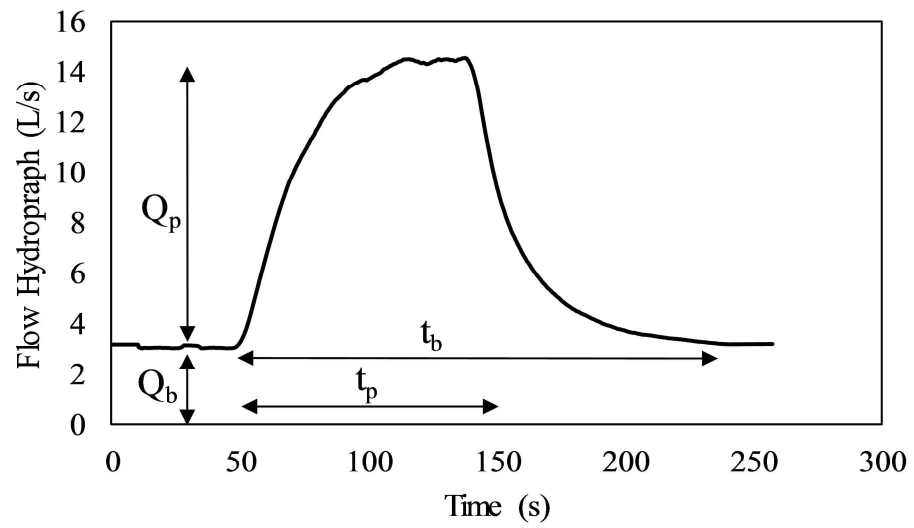


Figure 2. Experimental setup used to collect the unsteady flow data in the 595 mm PVC pipe.



665

666

Figure 3. Variable definition of the flushing discharge hydrograph.

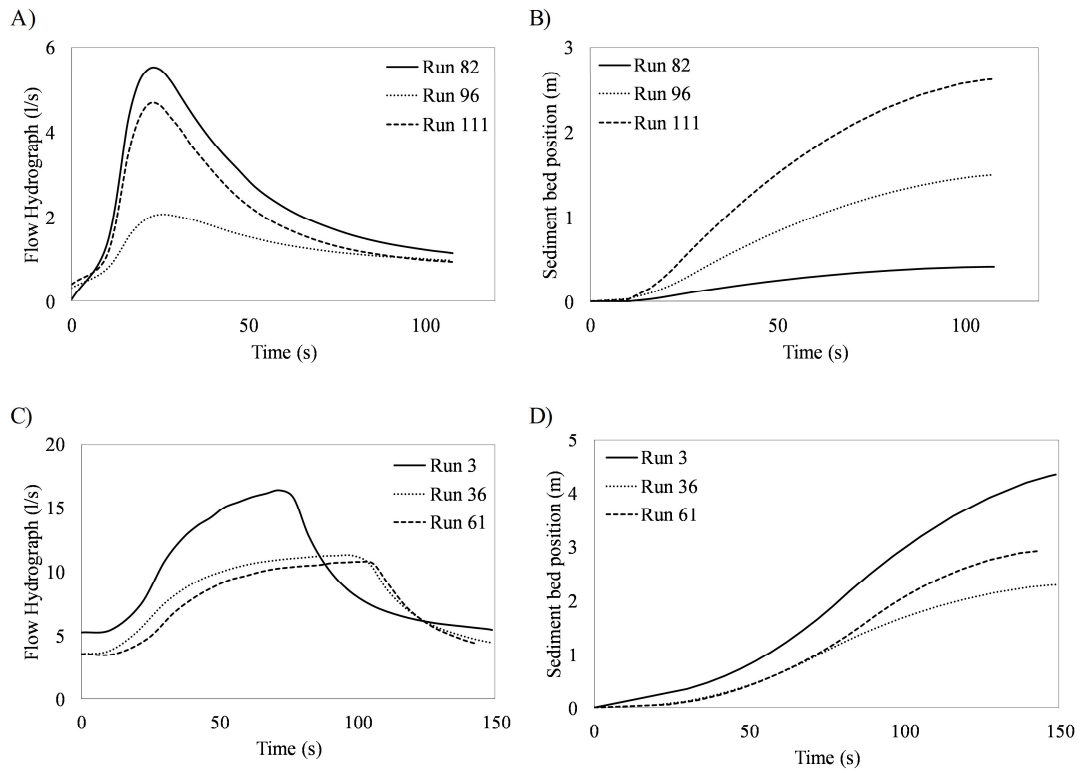


Figure 4. Example of flow hydrographs and sediment bed position for several experiments shown in Table 1.

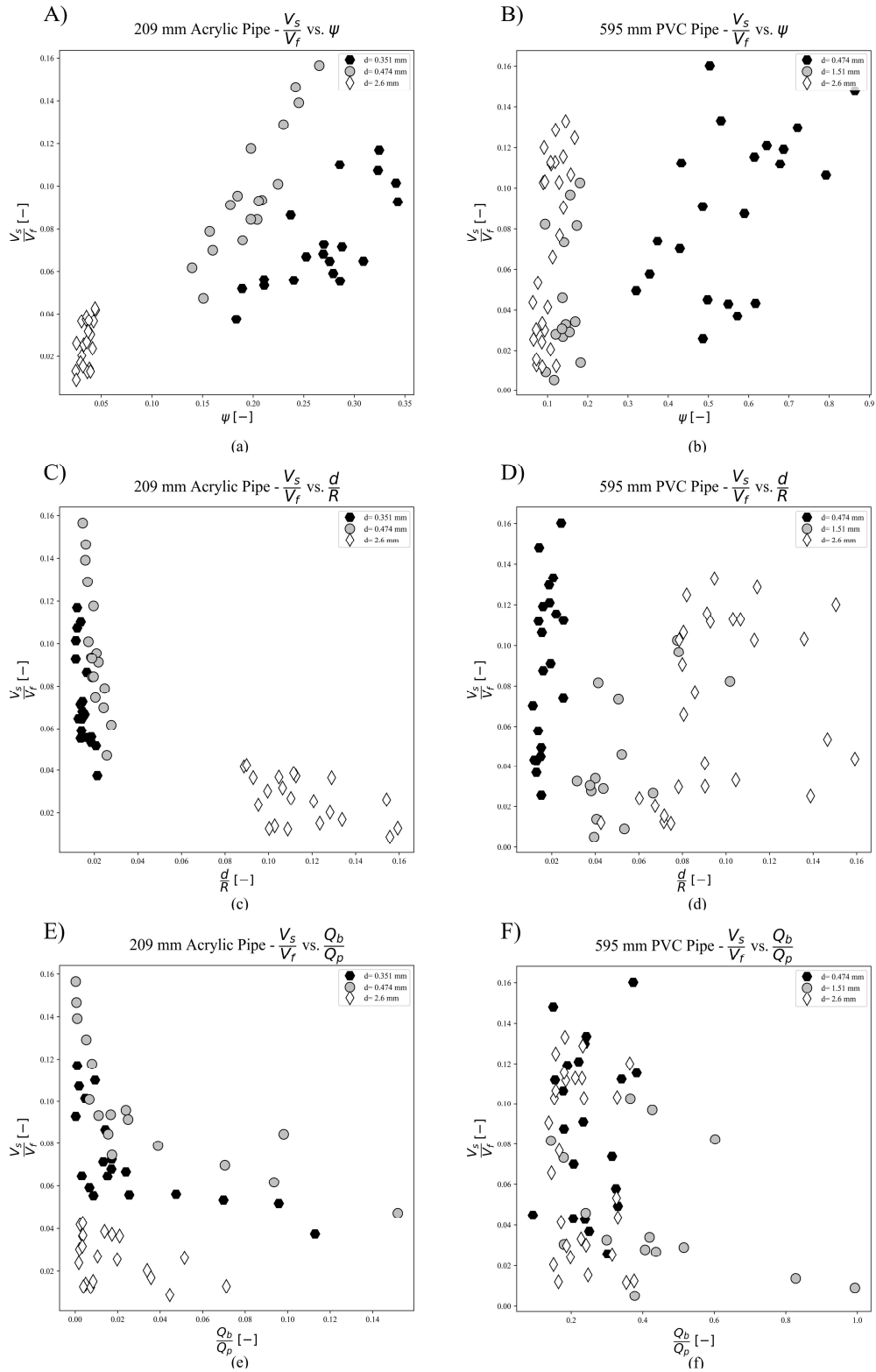


Figure 5. Plots showing the relationships between the dimensionless velocity (V_s/V_f) and other dimensionless variables in both acrylic and PVC pipe. Clustered results by particle diameter.

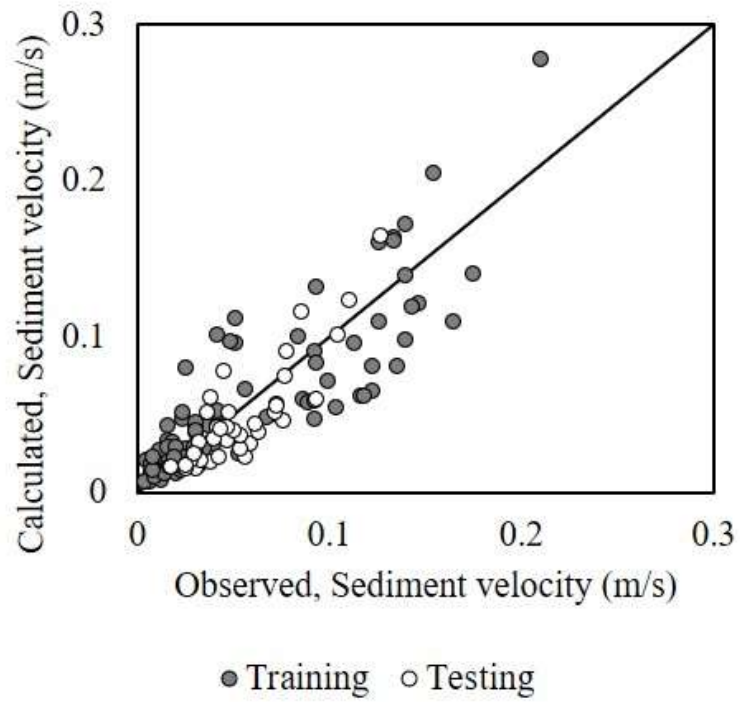


Figure 6. EPR-MOGA model accuracy for both training and testing stage.

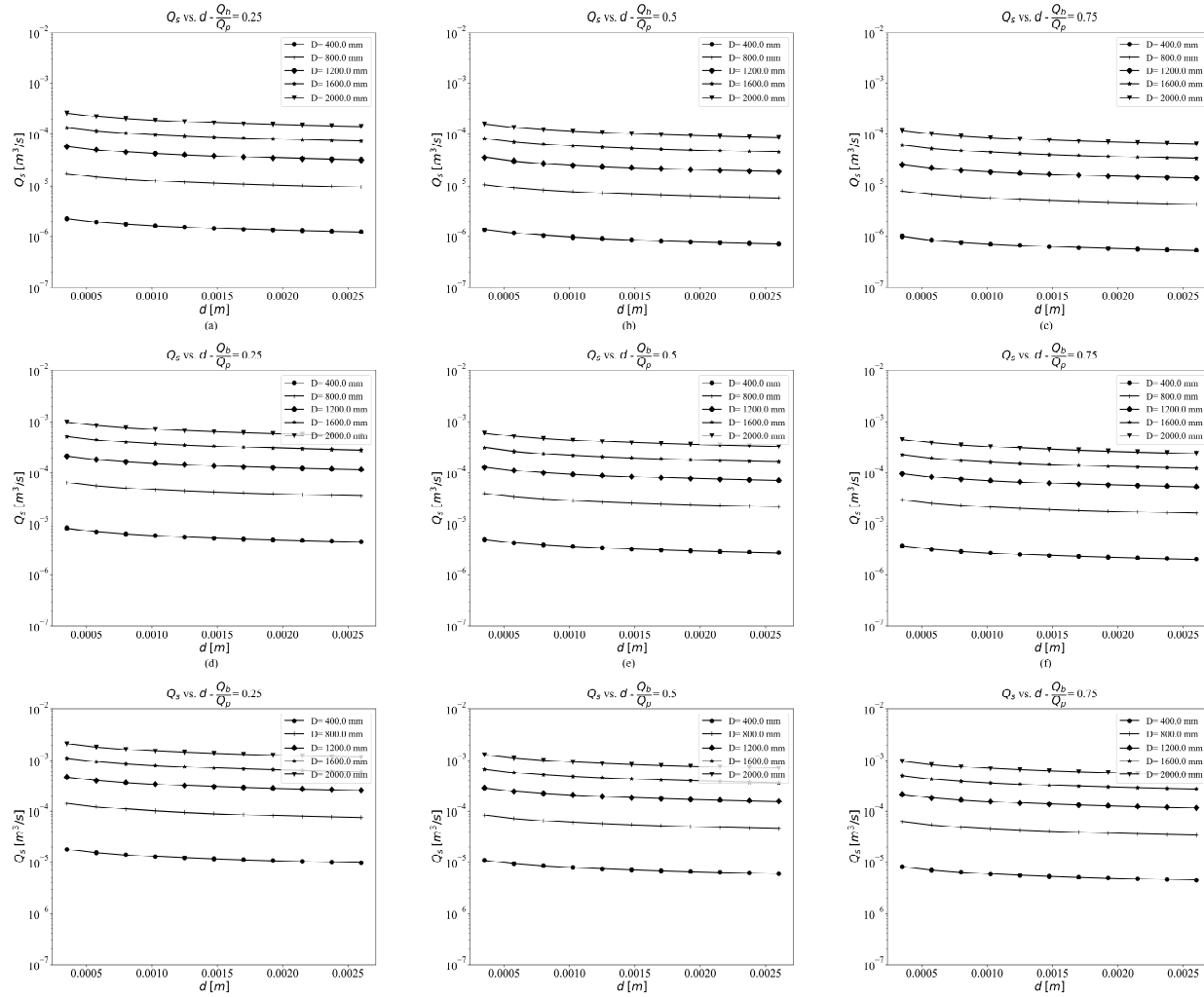


Figure 7. Efficiency of flushing discharge vs particle diameter for several base and peak flow relations ($0.25 < Q_b/Q_p < 0.75$) and pipe slope: a), b) and c) $S_o = 0.5\%$; d), e) and f) $S_o = 1.0\%$ and g), h) and i) $S_o = 1.5\%$.

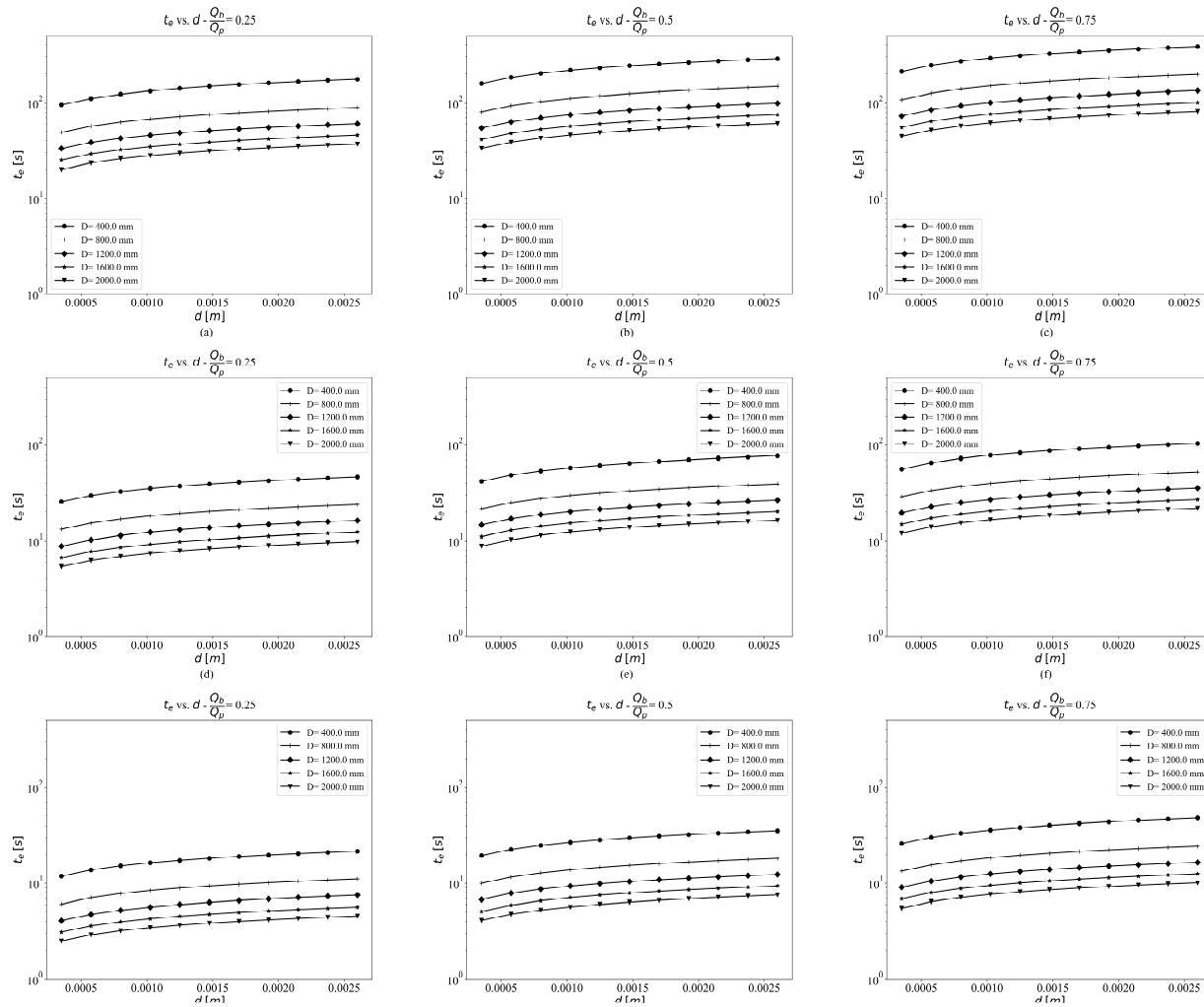


Figure 8. Flushing time vs particle diameter for several base and peak flow relations ($0.25 < Q_b/Q_p < 0.75$) and pipe slope: a), b) and c) $S_o = 0.5\%$; d), e) and f) $S_o = 1.0\%$ and g), h) and i) $S_o = 1.5\%$.

Table 1. Experimental data collected for studying flushing waves efficiency on sewer pipes.

Run no.	S_o (%)	D (mm)	Y (mm)	R (mm)	d (mm)	SG (-)	y_s (mm)	t_b (s)	t_p (s)	Q_b (l s ⁻¹)	Q_p (l s ⁻¹)	V_f (m s ⁻¹)	V_s (m s ⁻¹)
1	0.805	595	70.35	41.96	0.47	2.66	10.14	154	59	5.27	25.48	1.02	0.07
2	0.805	595	57.43	34.62	0.47	2.66	8.26	141	57	5.45	16.76	0.89	0.05
3	0.805	595	53.61	31.34	0.47	2.66	10.53	131	57	5.45	16.49	0.82	0.04
4	1.186	595	57.82	36.46	0.47	2.66	2.49	121	59	4.89	20.53	1.20	0.05
5	1.229	595	54.70	31.17	0.47	2.66	12.55	115	55	4.81	15.97	0.99	0.03
6	1.229	595	61.66	36.67	0.47	2.66	9.91	120	55	5.07	20.27	1.14	0.04
7	1.229	595	50.94	31.92	0.47	2.66	3.90	183	58	1.03	11.10	1.09	0.05
8	1.229	595	67.63	39.54	0.47	2.66	12.15	124	57	5.03	24.47	1.19	0.05
9	1.229	595	62.04	37.24	1.51	2.66	8.97	39	33	9.98	12.06	1.16	0.02
10	1.525	595	42.69	22.71	1.51	2.66	13.54	117	58	5.17	11.84	0.87	0.02
11	2.034	595	37.55	19.29	1.51	2.66	13.28	111	59	4.92	11.54	0.89	0.09
12	2.331	595	35.95	19.45	1.51	2.66	10.96	182	57	3.99	10.93	0.97	0.10
13	0.763	595	67.43	38.31	1.51	2.66	14.87	113	56	4.42	11.71	0.90	0.00
14	0.763	595	70.23	39.60	1.51	2.66	15.99	126	69	9.13	22.46	0.92	0.03
15	0.763	595	81.75	47.82	1.51	2.66	13.12	135	63	9.40	31.43	1.07	0.04
16	1.123	595	58.13	34.59	1.51	2.66	9.55	118	60	9.23	17.93	1.04	0.03
17	1.123	595	64.66	37.76	1.51	2.66	11.97	118	57	9.37	22.36	1.10	0.04
18	1.186	595	57.59	29.85	1.51	2.66	19.13	149	79	3.59	20.04	0.92	0.07
19	1.186	595	52.88	28.98	1.51	2.66	14.70	149	88	3.95	16.45	0.91	0.04
20	1.186	595	64.30	36.57	1.51	2.66	14.31	195	93	3.51	24.52	1.09	0.09
21	0.847	595	69.70	40.25	1.51	2.66	13.64	185	55	3.72	20.71	0.99	0.03
22	0.847	595	51.24	28.32	1.51	2.66	13.83	104	8	7.28	7.33	0.76	0.01
23	1.589	595	32.25	14.83	1.51	2.66	14.35	118	82	4.36	7.24	0.65	0.05
24	0.847	595	63.16	36.41	2.60	2.64	12.98	120	76	4.71	12.53	0.92	0.01
25	0.847	595	66.11	36.30	2.60	2.64	17.48	156	86	4.10	16.57	0.90	0.01
26	0.847	595	72.84	43.20	2.60	2.64	10.93	161	83	4.13	20.88	1.06	0.03
27	0.847	595	105.64	61.10	2.60	2.64	15.39	167	65	4.11	24.98	1.34	0.02
28	1.059	595	62.36	34.80	2.60	2.64	15.48	143	75	4.22	11.91	0.99	0.01
29	1.059	595	54.15	28.78	2.60	2.64	16.77	154	83	4.02	16.63	0.85	0.03
30	1.186	595	59.13	33.26	2.60	2.64	14.30	143	67	3.69	19.77	1.01	0.03
31	1.186	595	67.08	38.56	2.60	2.64	13.76	148	74	3.57	23.71	1.14	0.02
32	1.483	595	39.34	18.73	2.60	2.64	16.36	176	88	3.45	10.96	0.73	0.02

Run no.	S_o (%)	D (mm)	Y (mm)	R (mm)	d (mm)	SG (-)	y_s (mm)	t_b (s)	t_p (s)	Q_b (l s ⁻¹)	Q_p (l s ⁻¹)	V_f (m s ⁻¹)	V_s (m s ⁻¹)
33	1.483	595	46.74	24.88	2.60	2.64	14.66	136	80	3.52	15.45	0.91	0.03
34	1.483	595	53.25	28.81	2.60	2.64	15.54	186	72	3.39	19.73	1.01	0.04
35	1.483	595	59.57	32.28	2.60	2.64	16.95	184	79	3.42	23.61	1.10	0.07
36	1.653	595	38.51	16.34	2.60	2.64	19.13	134	82	3.75	11.36	0.69	0.03
37	1.653	595	46.08	23.02	2.60	2.64	17.21	141	84	3.76	15.96	0.90	0.09
38	1.653	595	52.56	28.02	2.60	2.64	16.18	146	70	3.71	20.08	1.04	0.12
39	1.653	595	59.13	33.13	2.60	2.64	14.58	147	64	3.64	23.79	1.19	0.12
40	1.568	595	38.73	18.76	0.47	2.66	15.60	135	87	3.64	11.58	0.76	0.06
41	1.568	595	46.16	24.41	0.47	2.66	14.80	142	81	3.73	15.96	0.92	0.08
42	1.568	595	53.90	29.62	0.47	2.66	14.77	146	87	3.66	20.35	1.07	0.09
43	1.568	595	59.10	34.08	0.47	2.66	12.39	151	81	3.75	24.25	1.20	0.13
44	1.822	595	37.55	18.70	0.47	2.66	14.29	140	87	4.06	11.92	0.82	0.09
45	1.822	595	45.29	22.96	0.47	2.66	16.33	148	88	4.00	16.48	0.95	0.13
46	1.822	595	51.59	29.70	0.47	2.66	11.33	152	81	3.95	20.87	1.17	0.14
47	2.034	595	35.08	19.49	0.47	2.66	9.71	121	84	3.97	10.64	0.92	0.15
48	2.034	595	42.85	24.99	0.47	2.66	9.05	161	89	3.26	14.75	1.11	0.13
49	2.034	595	50.35	30.68	0.47	2.66	6.79	7	78	3.56	20.07	1.32	0.14
50	2.034	595	54.22	33.47	0.47	2.66	5.64	178	60	3.56	23.79	1.42	0.21
51	2.246	595	34.90	21.54	0.47	2.66	4.68	127	75	4.36	11.38	1.09	0.13
52	2.246	595	42.64	25.31	0.47	2.66	7.95	159	77	3.78	15.90	1.19	0.15
53	2.246	595	35.17	17.28	2.60	2.64	13.82	131	78	4.07	11.19	0.86	0.10
54	2.246	595	42.78	22.75	2.60	2.64	13.58	142	88	3.62	15.55	1.06	0.14
55	2.246	595	47.24	27.46	2.60	2.64	9.96	146	85	3.62	19.82	1.24	0.17
56	2.246	595	52.77	31.74	2.60	2.64	8.10	142	79	3.72	23.74	1.40	0.18
57	2.076	595	36.93	19.14	2.60	2.64	12.77	136	85	3.90	11.87	0.90	0.09
58	2.076	595	43.16	24.38	2.60	2.64	10.84	11	77	3.69	16.02	1.09	0.12
59	2.076	595	50.20	28.50	2.60	2.64	11.99	153	92	3.67	20.34	1.21	0.14
60	2.076	595	54.70	32.31	2.60	2.64	9.85	154	79	3.79	24.16	1.35	0.14
61	1.822	595	36.34	17.74	2.60	2.64	14.46	123	84	3.54	10.84	0.79	0.04
62	1.822	595	43.56	25.20	2.60	2.64	9.63	162	85	3.20	15.12	1.05	0.12
63	1.822	595	50.97	30.34	2.60	2.64	8.79	171	78	3.18	19.05	1.21	0.09
64	1.822	595	56.21	32.54	2.60	2.64	11.66	168	87	3.25	23.71	1.25	0.11
65	0.644	209	34.99	20.17	2.60	2.64	5.60	101	18	0.08	3.80	0.55	0.02
66	0.644	209	49.27	27.29	2.60	2.64	8.22	101	16	0.01	6.60	0.68	0.02

Run no.	S_o (%)	D (mm)	Y (mm)	R (mm)	d (mm)	SG (-)	y_s (mm)	t_b (s)	t_p (s)	Q_b (l s ⁻¹)	Q_p (l s ⁻¹)	V_f (m s ⁻¹)	V_s (m s ⁻¹)
67	0.644	209	51.63	27.99	2.60	2.64	9.89	101	14	0.02	6.84	0.68	0.02
68	0.644	209	28.15	16.32	2.60	2.64	4.98	101	20	0.14	1.99	0.48	0.01
69	0.644	209	30.78	16.70	2.60	2.64	7.96	101	19	0.11	2.45	0.47	0.00
70	0.644	209	40.49	23.10	2.60	2.64	6.26	101	17	0.08	4.73	0.61	0.02
71	0.644	209	53.26	29.33	2.60	2.64	8.49	101	15	0.02	7.37	0.71	0.03
72	0.644	209	35.58	20.28	2.60	2.64	6.26	101	20	0.12	3.62	0.55	0.01
73	0.644	209	40.61	23.32	2.60	2.64	5.82	101	18	0.06	4.58	0.62	0.02
74	0.644	209	45.95	25.29	2.60	2.64	8.76	101	17	0.03	5.42	0.64	0.01
75	0.644	209	52.17	28.92	2.60	2.64	7.96	101	16	0.03	7.22	0.71	0.03
76	0.644	209	29.87	16.87	2.60	2.64	6.26	101	21	0.11	2.06	0.48	0.01
77	0.644	209	33.61	19.44	2.60	2.64	5.39	101	19	0.10	2.75	0.54	0.01
78	0.644	209	44.28	24.82	2.60	2.64	7.45	101	18	0.02	5.17	0.64	0.02
79	0.644	209	47.12	26.13	2.60	2.64	8.22	101	18	0.01	5.90	0.66	0.02
80	0.644	209	38.03	21.54	2.60	2.64	6.72	101	19	0.08	3.80	0.58	0.01
81	0.644	209	41.49	23.59	2.60	2.64	6.49	101	18	0.05	4.59	0.62	0.02
82	0.644	209	43.13	23.90	2.60	2.64	8.22	101	17	0.04	5.55	0.61	0.01
83	0.644	209	44.99	24.43	2.60	2.64	9.60	101	16	0.02	6.11	0.62	0.02
84	0.644	209	38.93	21.05	2.60	2.64	9.31	101	18	0.04	4.51	0.55	0.01
85	0.644	209	47.10	25.93	2.60	2.64	8.76	101	17	0.02	5.83	0.65	0.01
86	0.644	209	38.30	22.59	0.47	2.66	3.91	101	17	0.10	4.36	0.62	0.06
87	0.644	209	51.25	29.60	0.47	2.66	3.68	101	16	0.00	7.36	0.76	0.11
88	0.644	209	52.44	29.99	0.47	2.66	4.65	101	15	0.01	7.64	0.75	0.10
89	0.644	209	29.07	17.09	0.47	2.66	4.40	101	19	0.21	2.22	0.50	0.03
90	0.644	209	33.05	19.59	0.47	2.66	3.91	101	17	0.19	2.65	0.56	0.04
91	0.644	209	41.19	24.21	0.47	2.66	3.86	101	18	0.04	4.99	0.65	0.08
92	0.644	209	56.85	32.46	0.47	2.66	3.51	101	15	0.00	8.02	0.81	0.13
93	0.644	209	39.63	23.20	0.47	2.66	4.40	101	17	0.07	4.08	0.62	0.05
94	0.644	209	43.42	25.52	0.47	2.66	3.46	101	17	0.08	4.99	0.68	0.06
95	0.644	209	47.40	27.47	0.47	2.66	4.21	101	16	0.04	5.56	0.71	0.07
96	0.644	209	30.86	18.45	0.47	2.66	3.46	101	19	0.32	2.08	0.54	0.03
97	0.644	209	32.77	19.21	0.47	2.66	4.59	101	20	0.11	2.80	0.54	0.04
98	0.644	209	42.21	24.97	0.47	2.66	3.03	101	19	0.41	4.22	0.67	0.06
99	0.644	209	37.41	21.71	0.47	2.66	5.18	101	19	0.09	3.79	0.59	0.05
100	0.644	209	41.66	24.19	0.47	2.66	4.86	101	17	0.07	4.63	0.64	0.05

Run no.	S_o (%)	D (mm)	Y (mm)	R (mm)	d (mm)	SG (-)	y_s (mm)	t_b (s)	t_p (s)	Q_b (l s ⁻¹)	Q_p (l s ⁻¹)	V_f (m s ⁻¹)	V_s (m s ⁻¹)
101	0.644	209	43.34	25.14	0.47	2.66	4.78	101	18	0.06	5.71	0.66	0.06
102	0.644	209	48.65	28.13	0.47	2.66	4.21	101	16	0.03	6.67	0.72	0.09
103	0.644	209	36.32	21.27	0.35	2.65	4.59	101	18	0.06	4.24	0.58	0.05
104	0.644	209	51.00	29.01	0.35	2.65	5.60	101	15	0.01	6.81	0.73	0.08
105	0.644	209	50.99	29.11	0.35	2.65	5.18	101	15	0.01	6.90	0.73	0.09
106	0.644	209	28.62	16.45	0.35	2.65	5.39	101	18	0.23	2.00	0.48	0.02
107	0.644	209	32.66	18.92	0.35	2.65	5.26	101	17	0.19	2.67	0.53	0.03
108	0.644	209	42.79	24.72	0.35	2.65	5.18	101	16	0.07	4.80	0.65	0.04
109	0.644	209	54.41	30.76	0.35	2.65	5.60	101	17	0.00	7.36	0.76	0.07
110	0.644	209	37.13	21.55	0.35	2.65	5.18	101	18	0.10	3.75	0.59	0.03
111	0.644	209	41.56	24.21	0.35	2.65	4.59	101	17	0.08	4.71	0.64	0.05
112	0.644	209	45.08	25.81	0.35	2.65	5.73	101	17	0.07	5.47	0.67	0.05
113	0.644	209	54.08	30.60	0.35	2.65	5.60	101	15	0.03	7.31	0.76	0.08
114	0.644	209	29.46	16.96	0.35	2.65	5.39	101	20	0.19	2.02	0.49	0.03
115	0.644	209	33.04	18.92	0.35	2.65	5.90	101	19	0.13	2.74	0.53	0.03
116	0.644	209	44.81	25.64	0.35	2.65	5.82	101	17	0.04	5.18	0.66	0.04
117	0.644	209	48.43	27.71	0.35	2.65	5.39	101	17	0.02	5.88	0.70	0.05
118	0.644	209	39.31	22.65	0.35	2.65	5.60	101	18	0.09	3.92	0.60	0.04
119	0.644	209	41.99	24.16	0.35	2.65	5.60	101	17	0.08	4.59	0.63	0.04
120	0.644	209	43.59	25.04	0.35	2.65	5.60	101	18	0.04	5.64	0.65	0.04
121	0.644	209	44.65	25.62	0.35	2.65	5.60	101	17	0.06	6.12	0.66	0.07

Table 2. Pareto solution provided by the EPR-MOGA strategy.

Number of Inputs	Terms of monomial formula							Performance Index	
	Coefficient (a_j)	ψ	$\frac{Q_b}{Q_p}$	$\frac{d}{R}$	$\frac{y_s}{R}$	$\frac{t_b}{t_p}$	β	BIC	R^2
1	0.17	0.50	-	-	-	-	-	-48.21	0.38
2	0.14	0.60	-0.10	-	-	-	-	-66.19	0.48
3	8.13	1.40	-0.30	0.90	-	-	-	-104.55	0.63
4	11.47	1.50	-0.30	1.00	0.10	-	-	-100.56	0.64
5	121.48	2.10	-0.20	1.60	0.80	0.10	-	-96.49	0.64
6	2.48	1.40	-0.30	0.90	0.10	-0.20	1.00	-92.22	0.64

Table 3. Comparison of results for predicting the flushing efficiency in Laplace et al. (2003) case of study.

Reference	Removal rate [kg m ⁻³]	Observations
Laplace et al. (2003)	0.93	Original case of Study reported in a trunk combined sewer in Marseille, France
Dettmar (2007)	-	Volume of water value reported to clean a pipe section of 150 m long. Relevant parameters as pipe slope and particle diameter are not considered.
Bong et al. (2013)	0.21	Good approximation. Experimental model (Eq. (3)) obtained with a constant flume slope of 0.001.
EPR-MOGA Eq. (10)	0.4 – 1.25	Good performance for predicting the removal rate during flushing waves operation. Model consider relevant parameters as the mean particle diameter and the pipe geometry.